TECHNISCHE MECHANIK, Band 21, Heft 3, (2001), 191-205
Manuskripteingang: 30. August 2000

A Dynamic Model for Thick Plates with Time-dependent Boundary Conditions

Zeng Deshun, S. Schreiber, W. Hauger

In this paper a dynamic model for thick plates with dynamic boundary conditions is established. In addition to the influences of the bending the transverse shear deformation and the rotatory inertia has been included. The model also contains the effects of the transverse normal stress and the membrane forces. The equations presented in this paper can be reduced to those based on the Mindlin plate theory and the classical plate theory. The numerical results demonstrate that the influence of the transverse normal stress is quite significant for the dynamic response of thick plates with dynamic boundary conditions.

1 Introduction

Many structural problems are related to dynamic boundary conditions. For example, the edges of the structure may be subjected to dynamic displacement or force excitations. In these cases the boundary conditions of the associated boundary value problem are time–dependent. These problems are generally solved by the classical methods of separation of the variables, the Laplace integral transform or the boundary operator method.

Vibrations of beams with time–dependent boundary conditions were analyzed in Mindlin et al. (1950). Vibrations of plates with dynamic boundary conditions were studied by using the classical plate theory in Venkataramana et al. (1979) and the Mindlin plate theory in Reismann (1968), respectively. However, the classical plate theory based on the Kirchhoff assumptions (Love (1944)) cannot be expected to hold for plates whose thickness is large with respect to the span. Neither can it be employed to describe the dynamic behaviour of plates when the wave numbers are large. Therefore, in order to adequately describe the motion of plate–type structures, various improved theories of plates have been developed and established, see e. g. Mindlin (1951), Reissner (1945), Timoshenko et al. (1959), Altenbach (1996), Ambartsumian (1964), Sundera (1974), Donell (1976), Soedel (1981), Zeng (1987). For example, the Mindlin plate theory generalizes the normal line assumption to become the straight line assumption and it contains the influences of the transverse shear deformation and the rotatory inertia. It is able to describe a wider range of phenomena than the classical plate theory. However, the Mindlin plate theory is restricted to the analysis of only moderately thick plates because the effect of the transverse normal stress is neglected. In addition, the Mindlin plate theory also neglects the thickness change of the plate, as the classical plate theory does. This means that the transverse normal strain is not considered, which leads to the conclusion that the transverse normal stress and the transverse normal strain are equal to zero at the same time. According to the three–dimensional theory this is impossible. This obvious contradiction can be overcome by using the three–dimensional theory or improved theories where the thickness change is also considered, see e. g. Reddy et al. (1985), Kant et al. (1989), Krätzig (1993) and Zeng (1993). In this paper, a dynamic model for thick plates with dynamic boundary conditions is established. In addition to the influences of the bending the transverse shear deformation and the rotatory inertia has been included. It also contains the effects of the transverse normal stress and the membrane forces. The dynamic boundary conditions are transformed into an equivalent load vector and then the problem can be solved as in the case of homogeneous boundary conditions. The equations presented in this paper can be reduced to those deduced in Venkataramana et al. (1979) and Reismann (1968).

2 Kinematic and Constitutive Equations

The salient features of the plate geometry are shown in the Figs. 1a and 1b.

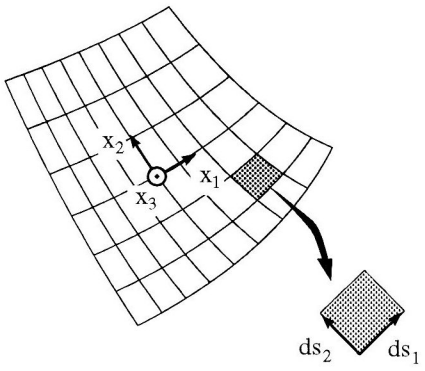

Figure 1a. Curvilinear Coordinate System

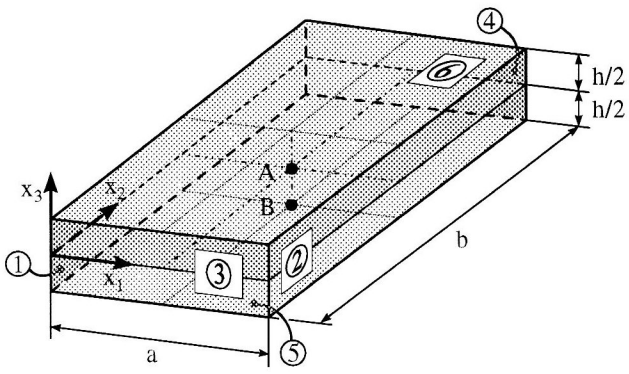

Figure 1b. Rectangular Plate used in the Numerical Analysis

The plate is referred to by a curvilinear orthogonal coordinate system x_1, x_2 and x_3, Fig. 1a. The axes x_1 and x_2 lie in the mid-surface of the plate, x_3 points into the direction of the normal to the mid-surface, forming a right hand coordinate system. The arc lengths are denoted by s_1 and s_2. One has the relations

$$\mathrm{d}\, s_1 = A_1\, \mathrm{d}\, x_1 \qquad\qquad \mathrm{d}\, s_2 = A_2\, \mathrm{d}\, x_2 \tag{1}$$

The quantities A_1 and A_2 are the coefficients of the first fundamental form of the mid-surface of the plate. These quantities are also referred to as g_{11} and g_{22} in the literature (since we restrict ourselves to an orthogonal coordinate system, the coefficient $A_{12} = g_{12} = 0$). For example, $A_1 = A_2 = 1$ for rectangular plates and $A_1 = 1$, $A_2 = r$ for circular plates (r denotes the radius).

We introduce the dimensions of the plate by $x_1 \in [0, a]$, $x_2 \in [0, b]$, $x_3 \in [-h/2, h/2]$; h denotes the thickness of the plate. The six faces ① to ⑥ are referred to by ① : $x_1 \equiv 0$, ② : $x_1 \equiv a$, ③ : $x_2 \equiv 0$, ④ : $x_2 \equiv b$, ⑤ : $x_3 \equiv -h/2$, and finally ⑥ : $x_3 \equiv h/2$. This notation implies that the respective coordinate is held at the given value while the other coordinates vary within their bounds. Fig. 1b shows a rectangular plate which is used later for the numerical analysis.

Considering the influences of the bending, the transverse shear deformation, the rotatory inertia, the effects of the transverse normal strain, and the membrane strains the displacement vector can be approximately taken as

$$\underline{u}^*(x_1, x_2, x_3, t) = \underline{u}(x_1, x_2, t) + x_3\, \underline{\varphi}(x_1, x_2, t) \tag{2}$$

with

$$\underline{u}^* = [u_1^*, u_2^*, u_3^*]^T \qquad \underline{u} = [u_1, u_2, u_3]^T \qquad \underline{\varphi} = [\varphi_1, \varphi_2, \varphi_3]^T \tag{3}$$

where $u_i (i = 1, 2, 3)$ are the displacement components of the mid-surface of the plate, φ_1 and φ_2 are the angles of rotation of the transverse normal in the $x_1 - x_3$ and $x_2 - x_3$ planes, φ_3 is the transverse normal strain (in this approach the transverse normal strain is linearly distributed over the height of the plate so that φ_3 is not a rotational degree of freedom), ^{T} denotes the transposition and t is the time.

The improved theory with six independent variables, the Mindlin plate theory with three independent variables (u_3, φ_1 and φ_2), and the classical plate theory with one independent variable (u_3) are hereafter denoted by IT6, MT3, and CT1, respectively. For better readability the following equations are given using substantial abbreviations, which are entirely written out in the appendix.

Using equation (2), the vector $\underline{e}^*$ which contains the normal strains and the shear strains can be computed by

$$\underline{e}^* = [e^*_{11}, e^*_{22}, e^*_{33}, e^*_{12}, e^*_{13}, e^*_{23}]^T = \begin{bmatrix} \underline{E}_{c11} & \underline{E}_{c12} \\ \underline{E}_{c21} & \underline{E}_{c22} \end{bmatrix} \begin{bmatrix} \underline{u} \\ \underline{\varphi} \end{bmatrix} \tag{4}$$

With the vector comprising the normal stresses and the shear stresses defined by

$$\underline{\sigma}^* = [\sigma^*_{11}, \sigma^*_{22}, \sigma^*_{33}, \sigma^*_{12}, \sigma^*_{13}, \sigma^*_{23}]^T \tag{5}$$

the three dimensional stress–strain relation is written as

$$\underline{\sigma}^* = \underline{D}^* \underline{e}^* \tag{6}$$

Using (4) and (6), we obtain the constitutive equations

$$\underline{n}_a = \begin{bmatrix} \underline{N}_{1u} & \underline{N}_{1\varphi} \\ \underline{N}_{2u} & \underline{N}_{2\varphi} \end{bmatrix} \begin{bmatrix} \underline{u} \\ \underline{\varphi} \end{bmatrix} \qquad \underline{m}_a = \begin{bmatrix} \underline{M}_{1u} & \underline{M}_{1\varphi} \\ \underline{M}_{2u} & \underline{M}_{2\varphi} \end{bmatrix} \begin{bmatrix} \underline{u} \\ \underline{\varphi} \end{bmatrix} \tag{7}$$

with

$$\underline{n}_a = [N_{11}, N_{22}, N_{33}, N_{12}, N_{21}, N_{13}, N_{23}]^T \tag{8}$$

$$\underline{m}_a = [M_{11}, M_{22}, M_{12}, M_{21}, M_{13}, M_{23}]^T \tag{9}$$

Here $\underline{n}_a$ and $\underline{m}_a$ are the stress and moment resultant vectors defined by

$$N_{ij} = \int_{-h/2}^{h/2} \sigma^*_{ij} \, \mathrm{d}x_3 \quad (i = 1,2,3 \text{ and } j = 1,2,3) \tag{10}$$

$$M_{ij} = \int_{-h/2}^{h/2} x_3 \, \sigma^*_{ij} \, \mathrm{d}x_3 \quad (i = 1,2 \text{ and } j = 1,2,3) \tag{11}$$

The symbols $\underline{N}_{iu}$, $\underline{N}_{i\varphi}$, $\underline{M}_{iu}$, $\underline{M}_{i\varphi}$ $(i = 1, 2)$ are the differential operator matrices, which depend on the modulus of elasticity E, the shear modulus G, Poisson's ratio ν, and the transverse shear correction factor $\kappa = \pi^2/12$ (Mirsky et al. (1957) and (1958)), see appendix. Please note that κ is needed in plate theories of up to 11 DOF. From 12 DOF onwards no more transverse shear correction is necessary. Yet in these higher order theories the moment resultant vector $\underline{m}_a$ obtains a seventh component M_{33} which is not present in the current model.

3 Variational Principle and Equations of Motion

The strain–energy density is expressed by

$$W^* = \frac{1}{2} \underline{\sigma}^{*T} \underline{e}^* \tag{12}$$

by means of which the strain energy of the plate is obtained by integration over the whole volume of the plate, which yields

$$W = \frac{1}{2} \int_0^a \int_0^b \int_{-h/2}^{h/2} \underline{\sigma}^{*T} \underline{e}^* A_1 A_2 \, \mathrm{d}x_3 \mathrm{d}x_2 \mathrm{d}x_1 \tag{13}$$

With the mass density ρ, the kinetic energy density is given by

$$T^* = \frac{1}{2}\rho \left(\frac{\partial}{\partial t}\underline{u}^*\right)^T \left(\frac{\partial}{\partial t}\underline{u}^*\right) \tag{14}$$

This is used to obtain the kinetic energy of the plate

$$T = \int_0^a \int_0^b \int_{-h/2}^{h/2} \frac{1}{2}\rho \left(\frac{\partial}{\partial t}\underline{u}^*\right)^T \left(\frac{\partial}{\partial t}\underline{u}^*\right) A_1 A_2 \, \mathrm{d}x_3 \mathrm{d}x_2 \mathrm{d}x_1 \tag{15}$$

Let f_i $(i = 1, 2, 3)$ denote the x_i–component of the external force per unit area $\underline{f}$ acting on the surface of the plate. The work done by this force is

$$W_e = \int_S \int \underline{f}^T \underline{u}^* \mathrm{d}S \tag{16}$$

with

$$\underline{f} = [f_1, f_2, f_3]^T \tag{17}$$

the integration being extended over the entire surface S of the plate.

The work done by the body force per unit volume

$$\underline{q} = [q_1, q_2, q_3]^T \tag{18}$$

where q_i $(i = 1, 2, 3)$ denotes the x_i–component of the body force, is

$$W_b = \int_V \int \int \underline{q}^T \underline{u}^* \, \mathrm{d}V \tag{19}$$

the integration being extended over the whole volume V of the plate.

Hamilton's principle

$$\delta \int_{t_1}^{t_2} L \, \mathrm{d}t = 0 \tag{20}$$

with the Lagrange function

$$L = T - [W - (W_e + W_b)] \tag{21}$$

is now applied to deduce the equations of motion as well as the appropriate boundary conditions. The general equations of motion for thick elastic plates with arbitrary shape take the following form

$$\begin{aligned} -J_0 \frac{\partial^2 u_i}{\partial t^2} + \frac{\partial}{\partial x_1}(N_{1i}A_2) + \frac{\partial}{\partial x_2}(N_{2i}A_1) + \tilde{N}_i + (N^*_{3i} + \bar{N}_i)A_1 A_2 &= 0 \\ -J_2 \frac{\partial^2 \varphi_i}{\partial t^2} + \frac{\partial}{\partial x_1}(M_{1i}A_2) + \frac{\partial}{\partial x_2}(M_{2i}A_1) + \tilde{M}_i + (N_{i3} + M^*_{3i} + \bar{M}_i)A_1 A_2 &= 0 \end{aligned} \tag{22}$$

with the abbreviations

$$J_0 = \rho A_1 A_2 h \qquad J_2 = \rho A_1 A_2 \frac{h^3}{12} \tag{23}$$

$$[N_{1i}^*, M_{1i}^*] = \int_{-h/2}^{h/2} [1, x_3] f_i \, \mathrm{d}x_3 \Big|_{① + ②} \qquad [N_{2i}^*, M_{2i}^*] = \int_{-h/2}^{h/2} [1, x_3] f_i \, \mathrm{d}x_3 \Big|_{③ + ④} \tag{24}$$

$$[N_{3i}^*, M_{3i}^*] = [1, x_3] \, f_i \Big|_{⑤ + ⑥} \tag{25}$$

$$[\bar{N}_i, \bar{M}_i] = \int_{-h/2}^{h/2} [1, x_3] \, q_i \, \mathrm{d}x_3 \qquad (i = 1, 2, 3) \tag{26}$$

$$\tilde{N}_i = N_{ij} \frac{\partial A_i}{\partial x_j} - N_{jj} \frac{\partial A_j}{\partial x_i} \qquad \tilde{M}_i = M_{ij} \frac{\partial A_i}{\partial x_j} - M_{jj} \frac{\partial A_j}{\partial x_i}$$

$$(i = 1, \ j = 2 \quad \text{and} \quad i = 2, \ j = 1)$$

$$\tilde{N}_3 = \tilde{M}_3 = 0 \tag{27}$$

The notation $\textcircled{k} + \textcircled{l}$ in the equations (24) and (25) should be simply read as *evaluated at the faces k and l and added.*

Using d'Alembert's principle and introducing the generalized displacement vector

$$\underline{v} = [\underline{u}^T, \underline{\varphi}^T] = [u_1, u_2, u_3, \varphi_1, \varphi_2, \varphi_3]^T \tag{28}$$

the equations of motion with damping can be written as

$$\underline{M} \, \ddot{\underline{v}} + \underline{C} \, \dot{\underline{v}} + \underline{K} \, \underline{v} = \underline{p} \tag{29}$$

Here, $\underline{p}$ is the generalized load vector, $\underline{M}$, $\underline{C}$, $\underline{K}$ are the mass matrix, the damping matrix, and the differential operator stiffness matrix, respectively, and dots denote differentiation with respect to the time t. While deducing (29), we made use of the Rayleigh assumption $\underline{C} = c_a \underline{M} + c_b \underline{K}$ with constants c_a, c_b. It is evident that equation (29) can be reduced to the equation deduced by Mindlin, if the effects of the transverse normal stress and the membrane forces are neglected. The boundary conditions are

$$u_i = 0 \ \text{ or } \ N_{ji} = N_{ji}^* \qquad \varphi_i = 0 \ \text{ or } \ M_{ji} = M_{ji}^* \qquad (i = 1, 2, 3) \tag{30}$$

for the boundaries $x_j = \text{const.}$ $(j = 1, 2)$. Also, the initial displacements and velocities

$$\underline{v}(x_1, x_2, t) \mid_{t=0} = \underline{v}_0(x_1, x_2) \qquad \dot{\underline{v}}(x_1, x_2, t) \mid_{t=0} = \dot{\underline{v}}_0(x_1, x_2) \tag{31}$$

with

$$\underline{v}_0 = [u_{10}, u_{20}, u_{30}, \varphi_{10}, \varphi_{20}, \varphi_{30}]^T \qquad \dot{\underline{v}}_0 = [\dot{u}_{10}, \dot{u}_{20}, \dot{u}_{30}, \dot{\varphi}_{10}, \dot{\varphi}_{20}, \dot{\varphi}_{30}]^T \tag{32}$$

must be specified.

4 Orthogonality Conditions for the Natural Mode Functions

An expression for the generalized displacement vector can be written in the following form for arbitrary wave numbers m and n

$$\underline{v}(x_1, x_2, t) = \sum_{m,n} \underline{v}_{mn}(x_1, x_2) \sin \omega_{mn} t \tag{33}$$

with

$$\underline{v}_{mn} = [U_{1mn}, U_{2mn}, U_{3mn}, \Phi_{1mn}, \Phi_{2mn}, \Phi_{3mn}]^T \tag{34}$$

Here U_{1mn} to Φ_{3mn} denote test functions in x_1 and x_2 for the respective degree of freedom (DOF). Since the model possesses six DOF, there exist in general six eigenfrequencies (branches) for every combination of the wave numbers m and n, see section 6. Hence, equation (33) implies a summation over $p = 1 \ldots 6$ for every term with index mn. Substitution of (33) into the equation for free vibrations without damping

$$\underline{M}\,\ddot{\underline{v}} + \underline{K}\,\underline{v} = 0 \tag{35}$$

and using the constitutive equations as well as homogeneous boundary conditions, leads to the orthogonality conditions for the natural mode functions

$$\mathcal{I}_{mnkl} \begin{cases} = 0 & \text{for} \quad m \neq k \quad \bigcup \quad n \neq l \\ \neq 0 & \text{for} \quad m = k \quad \bigcap \quad n = l \end{cases} \tag{36}$$

with

$$\mathcal{I}_{mnkl} = \int_0^a \int_0^b \underline{v}_{mn}^T \underline{M}\,\underline{v}_{kl}\,\mathrm{d}x_2 \mathrm{d}x_1 \tag{37}$$

5 Dynamic Response to Time-dependent Boundary Conditions

The dynamic boundary conditions corresponding to the above theoretical dynamic analysis model for thick plates can be described by

$$\begin{array}{lll} u_i(\textcircled{j},t) = \hat{u}_i(\textcircled{j}) f_i^{\textcircled{j}}(t) & \text{or} & N_{ki}(\textcircled{j},t) = \hat{N}_{ki}(\textcircled{j}) F_i^{\textcircled{j}}(t) \\ \varphi_i(\textcircled{j},t) = \hat{\varphi}_i(\textcircled{j}) f_{i+3}^{\textcircled{j}}(t) & \text{or} & M_{ki}(\textcircled{j},t) = \hat{M}_{ki}(\textcircled{j}) F_{i+3}^{\textcircled{j}}(t) \\ (i = 1,2,3;\ j = 1,2,3,4; & & k = 1 \text{ for } j = 1,2 \text{ and } 2 \text{ for } j = 3,4) \end{array} \tag{38}$$

Here $f_i^{\textcircled{j}}(t)$, $f_{i+3}^{\textcircled{j}}(t)$, $F_i^{\textcircled{j}}(t)$ and $F_{i+3}^{\textcircled{j}}(t)$ are prescribed functions of the time t while $\textcircled{j}$ denotes the face j as introduced in section 2. The key to the analysis lies in dealing with the dynamic boundary conditions. Making the dynamic boundary conditions homogeneous is a convenient and effective method to study the dynamic response. Therefore, we assume that the solution can be expressed by

$$\underline{v}(x_1,x_2,t) = \sum_{m,n} \underline{v}_{mn}(x_1,x_2) T_{mn}(t) + \sum_{r=1}^{r^*} \tilde{\underline{v}}_r(x_1,x_2,t) \qquad (r^* \leq 24) \tag{39}$$

where $\underline{v}_{mn}(x_1,x_2)$ satisfy the homogeneous boundary conditions and $\tilde{\underline{v}}_r(x_1,x_2,t)$ the dynamic ones. Then, $\tilde{\underline{v}}_r(x_1,x_2,t)$ can be chosen as

$$\tilde{\underline{v}}_r(x_1,x_2,t) = \hat{\underline{v}}_r(x_1,x_2) f_r(t) \tag{40}$$

with

$$\tilde{\underline{v}}_r = [\tilde{\underline{u}}_r, \tilde{\underline{\varphi}}_r]^T = [\tilde{u}_1^r, \tilde{u}_2^r, \tilde{u}_3^r, \tilde{\varphi}_1^r, \tilde{\varphi}_2^r, \tilde{\varphi}_3^r]^T \tag{41}$$

$$\hat{\underline{v}}_r = [\hat{\underline{u}}_r, \hat{\underline{\varphi}}_r]^T = [\hat{u}_1^r, \hat{u}_2^r, \hat{u}_3^r, \hat{\varphi}_1^r, \hat{\varphi}_2^r, \hat{\varphi}_3^r]^T \tag{42}$$

Substituting equation (39) into the equation of motion (29) gives

$$\begin{aligned} \underline{M}\,\frac{\partial^2}{\partial t^2}\left[\sum_{m,n} \underline{v}_{mn}(x_1,x_2) T_{mn}(t)\right] \quad &+ \quad \underline{C}\,\frac{\partial}{\partial t}\left[\sum_{m,n} \underline{v}_{mn}(x_1,x_2) T_{mn}(t)\right] \\ + \underline{K}\left[\sum_{m,n} \underline{v}_{mn}(x_1,x_2) T_{mn}(t)\right] \quad &= \quad \underline{p} + \tilde{\underline{p}} \end{aligned} \tag{43}$$

with

$$\underline{\tilde{p}} = -\left[\underline{M}\,\frac{\partial^2}{\partial t^2}\sum_{r=1}^{r^*}\tilde{\underline{v}}_r(x_1,x_2,t) + \underline{C}\,\frac{\partial}{\partial t}\sum_{r=1}^{r^*}\tilde{\underline{v}}_r(x_1,x_2,t) + \underline{K}\sum_{r=1}^{r^*}\tilde{\underline{v}}_r(x_1,x_2,t)\right] \tag{44}$$

Hence, the dynamic boundary conditions are transformed into an equivalent load vector $\underline{\tilde{p}}$ and the problem reduces to the solution of equation (43) with homogeneous boundary conditions. Using the orthogonality conditions for the natural mode functions, the dynamic response to the dynamic boundary conditions becomes

$$\begin{aligned}\underline{v}(x_1,x_2,t) = &\\ &\sum_{m,n}\underline{v}_{mn}(x_1,x_2)\left\{\mathrm{e}^{-\epsilon_{mn}t}\left[T_{mn}(0)\cos\omega^*_{mn}t + \frac{\dot{T}_{mn}(0)+\epsilon_{mn}T_{mn}(0)}{\omega^*_{mn}}\sin\omega^*_{mn}t\right]\right.\\ &\left.+\frac{1}{\omega^*_{mn}}\int_0^t \mathrm{e}^{-\epsilon_{mn}(t-\tau)}\left[P_{mn}(\tau)+\tilde{P}_{mn}(\tau)\right]\sin\omega^*_{mn}(t-\tau)\,\mathrm{d}\tau\right\} + \sum_{r=1}^{r^*}\tilde{\underline{v}}_r(x_1,x_2,t)\end{aligned} \tag{45}$$

with

$$\zeta_{mn} = \frac{c_a + c_b\omega^2_{mn}}{2\omega_{mn}}, \quad \epsilon_{mn} = \zeta_{mn}\omega_{mn}, \quad \omega^*_{mn} = \omega_{mn}\sqrt{1-\zeta^2_{mn}} \tag{46}$$

and

$$\left[P_{mn}(t),\tilde{P}_{mn}(t)\right] = \frac{1}{\mathcal{I}_{mnmn}}\int_0^a\int_0^b \left[\underline{p}^T(x_1,x_2,t),\underline{\tilde{p}}^T(x_1,x_2,t)\right]\ \underline{M}\ \underline{v}_{mn}(x_1,x_2)\,\mathrm{d}x_2\mathrm{d}x_1 \tag{47}$$

as well as

$$\begin{bmatrix} T_{mn}(0) \\ \dot{T}_{mn}(0)\end{bmatrix} = \frac{1}{\mathcal{I}_{mnmn}}\int_0^a\int_0^b\left\{\begin{bmatrix}\underline{v}_0^T\underline{M}\,\underline{v}_{mn}\\ \underline{\dot{v}}_0^T\underline{M}\,\underline{v}_{mn}\end{bmatrix} - \sum_{r=1}^{r^*}\underline{\hat{v}}_r^T\underline{M}\,\underline{v}_{mn}\begin{bmatrix} f_r(0)\\ \dot{f}_r(0)\end{bmatrix}\right\}\mathrm{d}x_2\mathrm{d}x_1 \tag{48}$$

The general expression of the solution shown in (45) can be reduced to the expressions deduced in Venkataramana et al. (1979) and Reismann (1968).

6 Numerical Results

Numerical computations based on the improved theory with six independent variables were carried out and compared to the results obtained by the classical theory. As an example, we consider the undamped vibrations of a simply supported plate initially at rest. Its edges are then subjected to harmonic displacement excitations perpendicular to the mid-surface. The boundary conditions are described by

$$\begin{aligned} &N_{11} = u_2 = M_{11} = \varphi_2 = 0 \quad u_3 = \hat{u}_3\sin\omega_a t \quad \varphi_3 = \hat{\varphi}_3\sin\omega_b t \qquad \text{(for the faces ①, ②)}\\ &N_{22} = u_1 = M_{22} = \varphi_1 = 0 \quad u_3 = \hat{u}_3\sin\omega_a t \quad \varphi_3 = \hat{\varphi}_3\sin\omega_b t \qquad \text{(for the faces ③, ④)}\end{aligned}$$

with the dimensionless amplitudes $\hat{u}_3$ and $\hat{\varphi}_3$.

The computations were performed using the following data:

- modulus of elasticity $E = 2.06 \times 10^5$ N/mm^2;
- Poisson's ratio $\nu = 0.3$;
- transverse shear correction factor $\kappa = \pi^2/12$;
- length to width ratios $a/b = 1.0,\ 4/3,\ 2$;

- thickness to length ratios $h/a = 0.01,\ 0.08,\ 0.2,\ 0.3$.

The symbols used are:

- fundamental frequency ω_0 of the plate (classical theory);
- wave numbers m and n in x_1 and x_2–direction;
- branch number p of the frequency (six branches for IT6, three branches for MT3 and one branch for CT1);
- non–dimensional frequency parameter $\Omega_{mnp} = \omega_{mnp}/\omega_0$;
- characteristic vector $\underline{ev}_{mnp} = [A_{mnp},\ B_{mnp},\ C_{mnp},\ D_{mnp},\ E_{mnp},\ F_{mnp}]^T$ for IT6, where A_{mnp} to F_{mnp} correspond to the independent kinematic quantities u_1, u_2, u_3, $\varphi_1 h/2$, $\varphi_2 h/2$, $\varphi_3 h/2$;
- non–dimensional characteristic vector $\underline{ev}^*_{mnp} = \underline{ev}_{mnp}/|\underline{ev}_{mnp}|$;
- frequencies ω_a, ω_b of the excitation;
- non–dimensional frequencies $\Omega_a = \omega_a/\omega_0 = 0.1$, $\Omega_b = \omega_b/\omega_0 = 0.1$;
- fundamental period T of the plate;
- non–dimensional diplacements $\tilde{u}_3 = 2u_3/u_0, \tilde{\varphi}_3 = h\varphi_3/u_0$, where u_0 denotes the static displacement in the x_3–direction at the centre of the plate subjected to the constant load P_0 by using CT1.

First we consider free vibrations. Table 1 shows examples of the non–dimensional frequency parameters and the non–dimensional characteristic vectors for a thin square plate based on IT6 for wave numbers $[m, n] = [1, 1]$. Terms of an absolute value less than $1 \cdot 10^{-4}$ are replaced by ε.

Table 1 $a/b = 1$ $h/a = 0.01$

Ω_{111}	Ω_{112}	Ω_{113}	Ω_{114}	Ω_{115}	Ω_{116}
0.9997	46.13	74.38	3262	3263	6079
$\underline{ev}^*_{111}$	$\underline{ev}^*_{112}$	$\underline{ev}^*_{113}$	$\underline{ev}^*_{114}$	$\underline{ev}^*_{115}$	$\underline{ev}^*_{116}$
0	-7,07E-01	7,07E-01	0	0	-1,57E-03
0	7,07E-01	7,07E-01	0	0	-1,57E-03
0,9998	0	0	ε	7,40E-03	0
-1,57E-02	0	0	-7,07E-01	7,07E-01	0
-1,57E-02	0	0	7,07E-01	7,07E-01	0
0	ε	6,67E-03	0	0	1-ε

Table 1. Non–dimensional Frequency Parameters and Non–dimensional Characteristic Vectors, a/b=1, h/a=0.01

None of the characteristic vectors contains more than three elements. Elements with an absolute value of more than 0.5, which predominate this mode, are shown in shaded cells. From the characteristic vectors it is apparent that IT6 can be divided into two separate mechanical submodels. This can in fact be shown analytically by inspection of the equation of motion (29). For the system under consideration the submodels are neither statically nor dynamically coupled. However, coupling occurs through external loading, see below. The first submodel represents the Mindlin plate theory (MT3), to which the third, fourth and fifth position in every characteristic vector for the branches $p = 1,\ 4,\ 5$ correspond. The second one contains the effects of the transverse normal stress and the membrane forces, to which the first, second and sixth position in every characteristic vector for the branches $p = 2,\ 3,\ 6$ belong. The frequencies for the branches $p = 4,\ 5$ and 6 correspond to the angles of rotation of the transverse normal and to the transverse normal strain. They are very high almost independent of the wave numbers m and n (the largest frequency parameter is more than 6000 times the smallest one in the case $m = n = 1$). This confirms the assumption that the effects of the transverse shear deformation, the rotatory inertia and the transverse normal stress are negligible for thin plates.

The results for the frequencies and the characteristic vectors for rectangular plates are given in the Tables 2–4.

Table 2 $a/b = 2$ $h/a = 0.08$

Ω_{281}	Ω_{282}	Ω_{283}	Ω_{284}	Ω_{285}	Ω_{286}
21,15	26,3	33,27	38,56	50,01	50,13
$\underline{ev}^*_{281}$	$\underline{ev}^*_{282}$	$\underline{ev}^*_{283}$	$\underline{ev}^*_{284}$	$\underline{ev}^*_{285}$	$\underline{ev}^*_{286}$
0	0,9923	0	6,37E-02	-6,03E-02	0
0	-1,24E-01	0	0,5096	-4,83E-01	0
0,9176	0	ε	0	0	1,43E-01
-4,93E-02	0	0,9923	0	0	1,23E-01
-3,94E-01	0	-1,24E-01	0	0	0,9821
0	ε	0	0,8580	0,8737	0

Table 2. Non–dimensional Frequency Parameters and Non–dimensional Characteristic Vectors, a/b=2, h/a=0.08

Table 3 $a/b = 2$ $h/a = 0.2$

Ω_{281}	Ω_{282}	Ω_{283}	Ω_{284}	Ω_{285}	Ω_{286}
9,325	10,52	11,01	11,07	17,93	18,19
$\underline{ev}^*_{281}$	$\underline{ev}^*_{282}$	$\underline{ev}^*_{283}$	$\underline{ev}^*_{284}$	$\underline{ev}^*_{285}$	$\underline{ev}^*_{286}$
0	0,9923	0	1,19E-02	1,19E-01	0
0	-1,24E-01	0	9,55E-02	0,9530	0
0,9757	0	ε	0	0	7,47E-02
-2,72E-02	0	0,9923	0	0	1,24E-01
-2,18E-01	0	-1,24E-01	0	0	0,9895
0	ε	0	0,9954	-2,79E-01	0

Table 3. Non–dimensional Frequency Parameters and Non–dimensional Characteristic Vectors, a/b=2, h/a=0.2

Table 4 $a/b = 2$ $h/a = 0.3$

Ω_{281}	Ω_{282}	Ω_{283}	Ω_{284}	Ω_{285}	Ω_{286}
6,294	6,838	7,012	7,161	11,89	11,98
$\underline{ev}^*_{281}$	$\underline{ev}^*_{282}$	$\underline{ev}^*_{283}$	$\underline{ev}^*_{284}$	$\underline{ev}^*_{285}$	$\underline{ev}^*_{286}$
0	7,33E-03	0,9923	0	1,22E-01	0
0	5,86E-02	-1,24E-01	0	0,9770	0
0,9982	0	0	ε	0	5,16E-02
-1,90E-02	0	0	0,9923	0	1,24E-01
-1,52E-01	0	0	-1,24E-01	0	0,9910
0	0,9983	ε	0	-1,75E-01	0

Table 4. Non–dimensional Frequency Parameters and Non–dimensional Characteristic Vectors, a/b=2, h/a=0.3

The wave numbers $m = 2$, $n = 8$ were arbitrarily chosen. Comparing these tables with Table 1 reveals some interesting phenomena. First, the ratio of the highest to the lowest eigenfrequency, $\Omega_{mn6}/\Omega_{mn1}$, decreases three orders in magnitude. Hence, there is a dense region of eigenfrequencies for an increasing ratio of thickness to span and increasing wave numbers. Secondly, the "positions" of the frequencies are shifted. While φ_3 is represented by the highest branch Ω_{116} for the thin square plate, its branch is shifted to the second position Ω_{282} for the thick rectangular plate. This leads to the conclusion that in this case the transverse normal strain plays a vital role and must not be neglected.

In the Figs. 2–4 the dynamic deflection of a square plate with different ratios of thickness to span subjected to the above dynamic boundary conditions is shown for the points A ($\tilde{u}_3$) and B ($\tilde{u}_3 - \tilde{\varphi}_3$), see Fig. 1b.

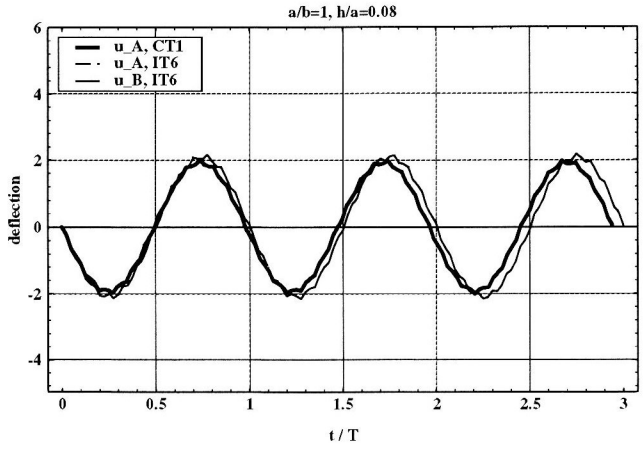

Figure 2. Normalized Deflection of the Points A and B vs. Time, a/b=1, h/a=0.08

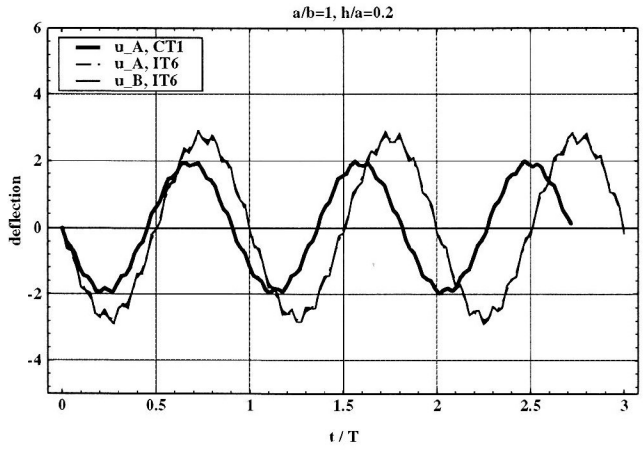

Figure 3. Normalized Deflection of the Points A and B vs. Time, a/b=1, h/a=0.2

As expected, the difference between CT1 and IT6 is almost negligible for the thin plate. However, with the increase of the ratio of thickness to span, both the amplitudes and the period of the responses increase for IT6. Because the higher order theory imposes less constraints (or renders more degrees of freedom) to the plate, it describes a softer system in general. The increasing differences between $\tilde{u}_A$ and $\tilde{u}_B$ are due to the effects of the tranverse normal strain.

For $h/a = 0.08$ and $h/a = 0.2$ the response described by CT1 features a seemingly harmonic shape, as it consists mainly of the first mode. The improved theory, however, reveals the influence of the additional branches, the eigenfrequencies of which lie within narrow bounds as mentioned above.

Figs. 5–7 show the same quantities for a rectangular plate. The very same effects are observed in an even amplified manner. It is obvious that the effects of the tranverse normal strain may not be neglected for thick plates.

Although we presented results only for dynamic *displacement* excitations of the boundaries, note that according to (38), studies on the effects of dynamic *force* excitations acting at the boundaries are feasible as well.

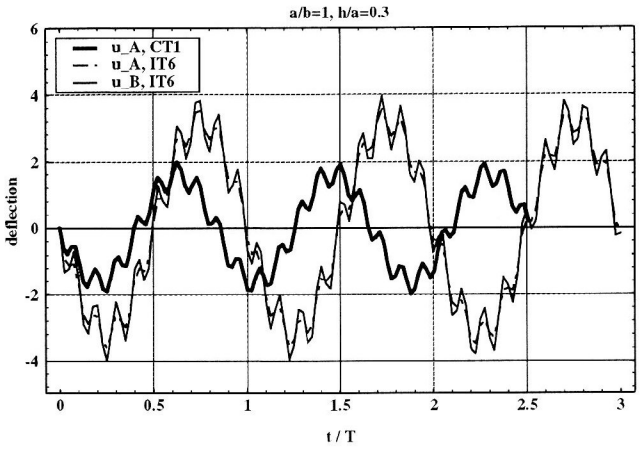

Figure 4. Normalized Deflection of the Points A and B vs. Time, a/b=1, h/a=0.3

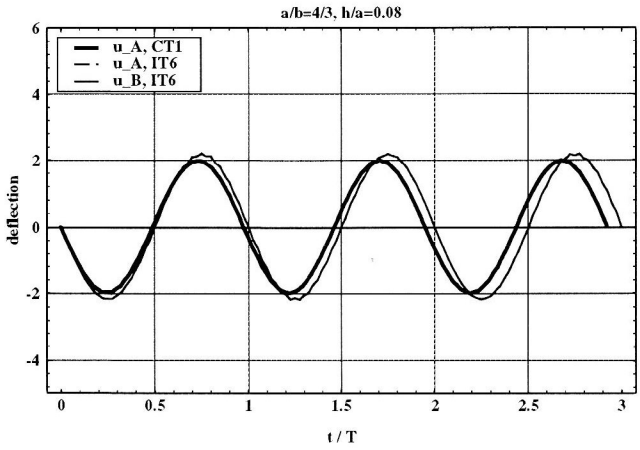

Figure 5. Normalized Deflection of the Points A and B vs. Time, a/b=4/3, h/a=0.08

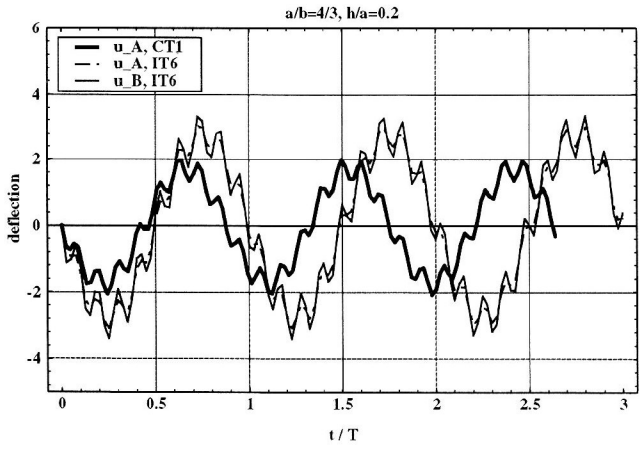

Figure 6. Normalized Deflection of the Points A and B vs. Time, a/b=4/3, h/a=0.2

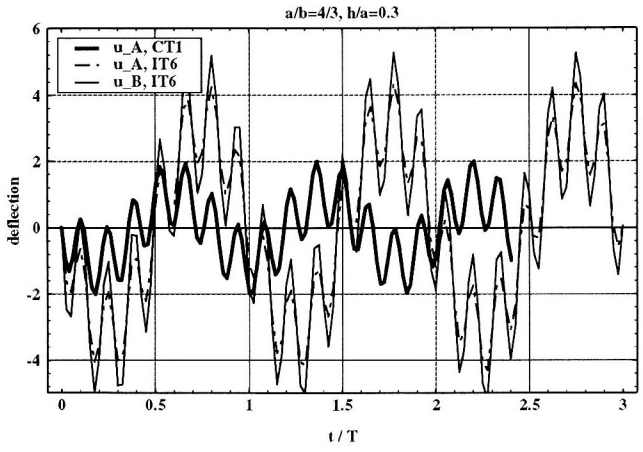

Figure 7. Normalized Deflection of the Points A and B vs. Time, a/b=4/3, h/a=0.3

7 Conclusions

We introduced a consistent plate theory with six independent variables and studied the response of a (thick) rectangular plate subjected to dynamic boundary conditions. The equivalent load vector $\underline{\tilde{p}}$, which represents the dynamic boundary conditions, plays the same role in inducing the response of plates as the generalized load vector $\underline{p}$ does, which represents the external loads. The following considerations therefore apply to both external loads and dynamic boundary conditions.

The improved model IT6 consists of two submodels, which comprise the MINDLIN plate (submodel 1, components u_3, φ_1 and φ_2) and a model containing the effects of the membrane forces and the transverse normal strain (submodel 2, components u_1, u_2, and φ_3). Inspection of the equations of motion yields that for the system under consideration these submodels are neither statically coupled through the stiffness matrix nor dynamically coupled through the mass matrix.

There is, however, a coupling of these submodels through the load vector in a way explained in the following. The force component f_3 naturally contributes to u_3 of the submodel 1. In addition, as an external force acts at the surface of the plate and not at the middle surface, this very component also excites φ_3 of the submodel 2. Therefore, through the intrinsic coupling in the submodels 1 and 2, all six DOF are excited.

Any tangential component f_1 or f_2 obviously contributes to u_1 and u_2, respectively. Again, as the component acts at the surface, it possesses a lever arm of $\pm h/2$, by means of which the bending DOFs φ_1 or φ_2 are excited. Now the same conclusion can be drawn, namely, that through the elastic coupling terms in the submatrices of $\underline{\mathrm{K}}$ again all six DOF are excited.

Since an oblique external force can always be decomposed into the above force components, it has been shown that there exists a coupling of the submodels 1 and 2 through the external load.

With the increase of the wave numbers as well as the ratio of thickness to span, dense regions of frequencies arise and the positions of the frequencies are shifted. The effect of the transverse normal stress grows with the increase of the ratio of thickness to span. As the classical plate theory and the moderately thick plate theory neglect the influence of the thickness change, the lower frequencies are lost in this case. The contributions of these frequencies on the dynamic response are also lost. Thus a large error can be caused. Therefore, not only the influences of the transverse shear deformation and the rotatory inertia, but also the effects of the transverse normal stresses must be included.

As lower order plate theories neglect the transverse normal stress and the transverse normal strain at the same time, one obtains a contradiction. The improved theory presented in this paper resolves this contradiction. Thus the range of application is extended to cover a broader scope. It must be kept in mind, though, that the theory introduced is still an approximation of the complete three–dimensional

theory. A rigid comparison between the three–dimensional theory and the current model has not been undertaken yet.

Acknowledgement

We gratefully acknowledge financial support by the Deutsche Forschungsgemeinschaft (DFG 446 CHV – 112/27/93).

Appendix

In the following, the complete expressions for the abbreviations introduced in section 2 are given. With the aid of these, the system matrices may be tailored for arbitrarily shaped plates.

Kinematic matrices:

$$\underline{E}_{c11} = \begin{bmatrix} \frac{1}{A_1}\frac{\partial}{\partial x_1} & \frac{1}{A_1 A_2}\frac{\partial A_1}{\partial x_2} & 0 \\ \frac{1}{A_1 A_2}\frac{\partial A_2}{\partial x_1} & \frac{1}{A_2}\frac{\partial}{\partial x_2} & 0 \\ 0 & 0 & 0 \end{bmatrix} \qquad \underline{E}_{c12} = \begin{bmatrix} \frac{x_3}{A_1}\frac{\partial}{\partial x_1} & \frac{x_3}{A_1 A_2}\frac{\partial A_1}{\partial x_2} & 0 \\ \frac{x_3}{A_1 A_2}\frac{\partial A_2}{\partial x_1} & \frac{x_3}{A_2}\frac{\partial}{\partial x_2} & 0 \\ 0 & 0 & 1 \end{bmatrix}$$

$$\underline{E}_{c21} = \begin{bmatrix} \left(\frac{1}{A_2}\frac{\partial}{\partial x_2} - \frac{1}{A_1 A_2}\frac{\partial A_1}{\partial x_2}\right) & \left(\frac{1}{A_1}\frac{\partial}{\partial x_1} - \frac{1}{A_1 A_2}\frac{\partial A_2}{\partial x_1}\right) & 0 \\ 0 & 0 & \frac{1}{A_1}\frac{\partial}{\partial x_1} \\ 0 & 0 & \frac{1}{A_2}\frac{\partial}{\partial x_2} \end{bmatrix}$$

$$\underline{E}_{c22} = \begin{bmatrix} x_3\left(\frac{1}{A_2}\frac{\partial}{\partial x_2} - \frac{1}{A_1 A_2}\frac{\partial A_1}{\partial x_2}\right) & x_3\left(\frac{1}{A_1}\frac{\partial}{\partial x_1} - \frac{1}{A_1 A_2}\frac{\partial A_2}{\partial x_1}\right) & 0 \\ 1 & 0 & \frac{x_3}{A_1}\frac{\partial}{\partial x_1} \\ 0 & 1 & \frac{x_3}{A_2}\frac{\partial}{\partial x_2} \end{bmatrix}$$

Symbols and matrices of the three–dimensional stress–strain relations ($\underline{I}$ denotes the identity matrix):

$$\underline{D}^* = \begin{bmatrix} \underline{D}_a^* & \underline{0} \\ \underline{0} & \underline{D}_b^* \end{bmatrix} \qquad \underline{D}_a^* = \begin{bmatrix} \lambda + 2G & \lambda & \lambda \\ \lambda & \lambda + 2G & \lambda \\ \lambda & \lambda & \lambda + 2G \end{bmatrix} \qquad \underline{D}_b^* = G\,\underline{I},$$

$$\lambda = \frac{E\nu}{(1+\nu)(1-2\nu)} \qquad G = \frac{E}{2(1+\nu)}$$

Differential operator matrices of the constitutive equations:

$$\underline{N}_{1u} = \begin{bmatrix} (\lambda + 2G)hD_{a11} + \lambda h D_{a21} & (\lambda + 2G)hD_{a12} + \lambda h D_{a22} & 0 \\ (\lambda + 2G)hD_{a21} + \lambda h D_{a11} & (\lambda + 2G)hD_{a22} + \lambda h D_{a12} & 0 \\ \lambda h\,(D_{a11} + D_{a21}) & \lambda h\,(D_{a12} + D_{a22}) & 0 \end{bmatrix}$$

$$\underline{N}_{2u} = \begin{bmatrix} Gh\,(D_{a22} - D_{a12}) & Gh\,(D_{a11} - D_{a21}) & 0 \\ Gh\,(D_{a22} - D_{a12}) & Gh\,(D_{a11} - D_{a21}) & 0 \\ 0 & 0 & \kappa G h D_{a11} \\ 0 & 0 & \kappa G h D_{a22} \end{bmatrix}$$

$$\underline{N}_{1\varphi} = \begin{bmatrix} 0 & 0 & \lambda h \\ 0 & 0 & \lambda h \\ 0 & 0 & (\lambda + 2G)h \end{bmatrix} \qquad \underline{N}_{2\varphi} = \begin{bmatrix} 0 & 0 & 0 \\ 0 & 0 & 0 \\ \kappa G h & 0 & 0 \\ 0 & \kappa G h & 0 \end{bmatrix}$$

$$\underline{M}_{1u} = \begin{bmatrix} 0 & 0 & 0 \\ 0 & 0 & 0 \end{bmatrix}$$

$$\underline{M}_{1\varphi} = \begin{bmatrix} (\lambda + 2G)\frac{h^3}{12} D_{a11} + \lambda \frac{h^3}{12} D_{a21} & (\lambda + 2G)\frac{h^3}{12} D_{a12} + \lambda \frac{h^3}{12} D_{a22} & 0 \\ (\lambda + 2G)\frac{h^3}{12} D_{a21} + \lambda \frac{h^3}{12} D_{a11} & (\lambda + 2G)\frac{h^3}{12} D_{a22} + \lambda \frac{h^3}{12} D_{a12} & 0 \end{bmatrix}$$

$$\underline{M}_{2u} = \begin{bmatrix} 0 & 0 & 0 \\ 0 & 0 & 0 \\ 0 & 0 & 0 \\ 0 & 0 & 0 \end{bmatrix} \qquad \underline{M}_{2\varphi} = \begin{bmatrix} G\frac{h^3}{12}(D_{a22} - D_{a12}) & G\frac{h^3}{12}(D_{a11} - D_{a21}) & 0 \\ G\frac{h^3}{12}(D_{a22} - D_{a12}) & G\frac{h^3}{12}(D_{a11} - D_{a21}) & 0 \\ 0 & 0 & \kappa G \frac{h^3}{12} D_{a11} \\ 0 & 0 & \kappa G \frac{h^3}{12} D_{a22} \end{bmatrix}$$

$$\underline{D}_a = \begin{bmatrix} \frac{1}{A_1}\frac{\partial}{\partial x_1} & \frac{1}{A_1 A_2}\frac{\partial A_1}{\partial x_2} & 0 \\ \frac{1}{A_1 A_2}\frac{\partial A_2}{\partial x_1} & \frac{1}{A_2}\frac{\partial}{\partial x_2} & 0 \end{bmatrix}$$

Literature

1. Altenbach, H.: On the Determination of Transverse Shear Stiffnesses of Orthotropic Plates, Z. angew. Math. Phys., (2000), 629–649.
2. Altenbach, H.; Altenbach, J.; Rikards, R.: Einführung in die Mechanik der Laminat– und Sandwichtragwerke, Stuttgart: Dt. Verl. für Grundstoffindustrie, ISBN 3–342–00681–1, (1996).
3. Ambartsumian, S. A.: Theory of Anisotropic Shells', Translation of "Teoriya anizotropnykh obolochek", Washington, D. C., National Aeronautics and Space Administration, (1964).
4. Carrera, E.: The Effects of Shear Deformation and Curvature on Buckling and Vibrations of Cross–Ply Laminated Composite Shells, J. of Sound and Vibration, 150, (1991), 405–433.
5. Donell, L. H.: Beams, Plates, and Shells, McGraw–Hill, New York, 1976.
6. Kant T.; Mallikarjuna: Vibrations of Unsymmetrically Laminated Plates Analyzed by Using a Higher Order Theory with a C^0 Finite Element Formulation, J. of Sound and Vibration, 134, (1989), 1–16.
7. Krätzig, W. B.: Bestmögliche innere Schalengleichungen für schubweiche Werkstoffe unter Berücksichtigung von Dickenänderungen, Ing.–Arch., 64, (1993), 1–19.
8. Landgraf, G. Berechnung beliebig belasteter Rotationsschalen mit und ohne Berücksichtigung des Querkraftschubs, Habilitationsschrift TU Dresden, (1969).
9. Love, A. E. H.: A Treatise on the Mathematical Theory of Elasticity, Dover Publications, New York, (1944).
10. Mindlin, R. D.: Influence of Rotatory Inertia and Shear on Flexural Motions of Isotropic Rectangular Plates, J. Appl. Mech., 18, (1951), 31–38.
11. Mindlin, R. D.; Goodman L. E.: Beam Vibrations with Time–dependent Boundary Conditions, J. of Appl. Mech., 17, (1950), 377–380.
12. Mirsky I.; Herrmann, G.: Nonaxially Symmetric Motion of Thick Cylindrical Shells', J. of Acoust. Soc. of America, (1957), 10–14.

13. Mirsky I.; Herrmann, G.: Axially Symmetric Motion of Thick Cylindrical Shells, J. of Applied Mechanics, (1958), 97–102.

14. Reddy, J. N.; Phan, N. S.: Stability and Vibration of Isotropic, Orthotropic and Laminated Plates according to a Higher–Order Shear Deformation Theory, J. of Sound and Vibration, 98, (1985), 157–170.

15. Reismann, H.: Forced Motion of Elastic Plates, Transactions of ASME, 35, (1968), 510–515.

16. Reissner, E.: The Effect of Transverse Shear Deformation on the Bending of Elastic Plates, J. Appl. Mech., 12, (1945), A69–A77.

17. Soedel, W.: Vibrations of Shells and Plates, M. Decker INC., New York and Basel, (1981).

18. Sundera Raja Iyengar, K. T.; Chandrashekhara K.; Sebastian, V. K.: On the Analysis of Thick Rectangular Plates, Ing.–Arch., 43, (1974), 317–330.

19. Timoshenko S. ; Woinowsky–Krieger, S.: Theory of Plates and Shells, McGraw–Hill, New York, (1959).

20. Ulbricht, V.: Physikalisch und geometrisch nichtlineare Schalentheorie in konvektiver Metrik, Habilitationsschrift TU Dresden, (1986).

21. Venkataramana, J.; Maiti, M.; Srinivasan, R. K.: Vibration of Rectangular Plates with Time–Dependent Boundary Conditions, J. of Sound and Vibration, 62, (1979), 327–337.

22. Zeng, D.: Die dynamische Analyse dicker Platten, Dissertation TU Dresden, (1987).

23. Zeng, D.: Die dynamische Analyse dicker Zylinderschalen, Habilitationsschrift TU Dresden, (1993).

Address: Prof. Dr.–Ing. habil. Zeng Deshun, Civil Engineering Key Technology, Tongji University, Shanghai 200092, PRC and Dr.–Ing. S. Schreiber, Prof. Dr. W. Hauger, Institut für Mechanik, TU Darmstadt, Hochschulstraße 1, D–64289 Darmstadt, Germany